energy&fuels

pubs.acs.org/EF

Article

Multistage Circulation Absorption Improvement: Simulation and Energy-Saving Evaluation of an Innovative Amine-Based CO_2 Capture Process

Chengjin Pan, Chang Liu, Lingyu Shao, Feng Xu, Zhicheng Wu, Zhengang Zhou, Xiao Zhang, Yang Zhang, Chenghang Zheng,* and Xiang Gao

Cite This: *Energy Fuels* 2024, 38, 2129−2140

Read Online

ACCESS | Metrics & More | Article Recommendations

ABSTRACT: High energy consumption poses a critical challenge in the context of postcombustion CO_2 capture (PCCC) processes. In this study, an innovative approach with a multistage circulation (MSC) process was proposed, which divided the absorber into three vertically arranged stages, each performing different functions, including CO_2 efficient capture, CO_2 absorption enhancement, and CO_2 enrichment. The analysis using the rate-based model in Aspen Plus was conducted. Compared to the conventional process, the MSC process resulted in an increase in the CO_2-cycling capacity and a reduction in regeneration duty. Several key parameters, including piperazine (PZ)/*N*-methyldiethanolamine (MDEA) ratio, CO_2 capture rate, intercooling temperature, CO_2 lean loading, and stripping pressure, underwent optimization. Additionally, modifications, such as rich solvent split and lean vapor recompression, led to a further decrease in regeneration duty. Through combining parameter optimization and process modification within the MSC framework, a low regeneration duty of 2.16 GJ/t CO_2 was achieved, a reduction of 28% compared to the conventional process. Correspondingly, the total equivalent work was reduced to 0.211 MW h/t of CO_2, representing a reduction of 11%. Finally, improvements for further reducing the regeneration duty based on the MSC process were proposed. This study has shown a novel method for designing PCCC system, offering important implications for achieving energy-efficient carbon capture.

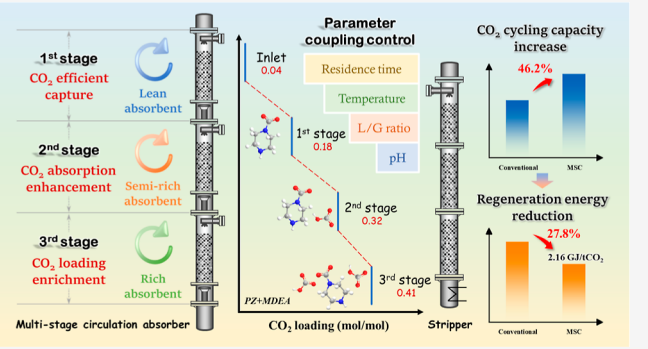

1. INTRODUCTION

The escalating level of CO_2 resulting from excessive emissions is widely acknowledged as a major contributor to global warming and climate change. The objective of the "Paris Agreement" is to constrain the increase in global average temperatures, ideally limiting it to 2 °C, preferably 1.5 °C.[1] In pursuit of this goal, CO_2 capture and valorization stand out as critical approaches toward achieving near-zero CO_2 emissions.[2] Among the various techniques, the amine-based chemical absorption and desorption of CO_2 represent the most commonly employed method for postcombustion CO_2 capture (PCCC) in coal-fired power plants.[3] However, the process of capturing CO_2 results in a substantial loss of overall electrical efficiency, amounting to nearly two-thirds of the total efficiency.[4] It is mainly due to the high energy consumption inherent in CO_2 desorption from amine solutions.[5] Therefore, it is significant to reduce the energy consumption associated with the CO_2 absorption process.

Developing low-energy absorbents is crucial for reducing the high energy consumption of the CO_2 capture process. Primary amines, for example, monoethanolamine (MEA), and secondary amines exhibit fast reaction kinetics with CO_2,[6] but require substantial energy input for regeneration due to the persistence of the carbamate stability.[7] In contrast, tertiary amines, for example, *N*-methyldiethanolamine (MDEA), do not react directly with CO_2, but facilitate the hydration of CO_2 to form bicarbonates.[8] Although tertiary amines typically have lower regeneration energy requirements, the application is limited by their comparatively slow reaction rates.[9] MEA, chosen widely as an amine-based absorbent in the PCCC process, has high chemical reactivity and good kinetic properties.[10] However, its application is hindered by the substantial regeneration energy requirement (~3.7 GJ/t CO_2),[11] as well as its propensity for corrosion and ease of

Received: October 24, 2023
Revised: December 20, 2023
Accepted: January 2, 2024
Published: January 17, 2024

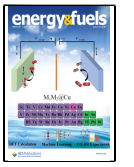

degradation.[12] The high regeneration duty in the MEA process primarily stems from the high absorption reaction heat of MEA, which is 87−93 kJ/mol CO_2.[13] Conversely, MDEA emerges as a potential candidate among these absorbents due to its lower reaction heat, measuring only 59−66 kJ/mol CO_2.[14] This characteristic positions MDEA as a potential option for energy-efficient PCCC processes. However, this advantage is offset by a slower CO_2 absorption rate, introducing an inevitable trade-off between augmenting absorption rate and minimizing energy consumption during regeneration.[15]

To address the limitations of single-amine CO_2 capture, blended amine solvents have been employed. These solvents usually consist of tertiary/sterically amines, characterized by low desorption reaction enthalpy and high cycling capacity, along with primary/secondary amines, characterized by fast absorption rates.[16] Sema et al.[17] showed that the addition of MEA positively influences reaction kinetics and enhances mass transfer performance. Another commonly utilized promoter is piperazine (PZ). Zhang et al.[18] demonstrated that blended systems containing MEA/MDEA/PZ exhibit higher CO_2 absorption capacity, faster CO_2 adsorption rate, and lower regeneration duties compared to the use of MEA alone. Additionally, various alternative absorbents have undergone extensive study. Zhang et al.[19] developed a dimethylcyclohexylamine-based two-phase absorbent that undergoes phase separation between 70 and 90 °C after CO_2 absorption, achieving a low regeneration energy of 2.50 GJ/t CO_2. Liu et al.[20] mixed 2-amino-2-methyl-1-propanol and MEA incorporating 50 wt % diethylene glycoldimethyl ether and yielded a regeneration energy of 2.70 GJ/t CO_2.

Blends of PZ and MDEA, with a well-established research foundation, have been extensively employed to assess the effectiveness of the CO_2 capture process. The vapor−liquid equilibrium model of the PZ−MDEA−CO_2−H_2O reaction system has been investigated by scholars.[21] It is worth noting that the reaction heat for CO_2 absorption by PZ is 83−88 kJ/mol CO_2, which is much higher than that reported for MDEA.[22] Research has shown that the blended PZ/MDEA solution exhibits an acceptable CO_2 absorption rate while maintaining a low regeneration duty.[23] Zhao et al.[24] achieved a reboiler duty of 2.74 GJ/t CO_2 through using a mixed 20/30 wt % PZ/MDEA solution and further reduced it to 2.24 GJ/t CO_2 by combining various process modifications. Khan et al.[25] investigated a mixed 15/35 wt % PZ/MDEA solution, achieving a reboiler duty of 2.44 GJ/t CO_2. However, these studies did not effectively demonstrate the advantage gained from the low reaction heat of the MDEA-based absorbents. Instead, the low absorption rate hinders the achievement of high CO_2-rich loadings. Increasing the absorption rate simply by increasing the PZ concentration leads to an inevitable increase in reaction heat accompanied by loss of PZ through volatilization. Therefore, it is necessary to develop new process enhancements to cater to absorbents with low regeneration energy requirements.

Optimizing the PCCC process involves enhancing the driving force for CO_2 mass transfer within the column and refining the heat utilization efficiency and system configuration.[26] These strategies aim to increase the CO_2-cycling capacity while minimizing the reboiler steam requirements, resulting in a reduction in the regeneration energy.[27] Researchers have developed a number of process modifications to improve CO_2 absorption and reduce regeneration duty, such as absorber intercooling (AIC),[28,29] rich solvent split (RSS),[24,30] lean vapor recompression (LVR),[29,31,32] rich solvent recycle (RSR),[26] and so on. Mostafavi et al.[29] conducted simulations to assess energy savings and costs associated with two different amine-based absorbents, MEA and PZ/MDEA, across a range of optimized configurations. Moullec et al.[26] cataloged and summarized the effects of 20 distinct fundamental modifications. For MDEA-based solvents, it is necessary to consider both the negative impact of the low CO_2 absorption rate and cycling capacity. Consequently, a comprehensive optimization of the process configuration becomes essential to match the specific absorbent properties.

Before extensive application of amine-based CO_2 capture processes, it is imperative to enhance the absorption efficiency and reduce energy consumption. Improvements to the process are essential to approach the theoretical maximum capacity of the absorbent, thereby minimizing energy consumption. In this study, an innovative multistage circulation (MSC) process was proposed to achieve energy-efficient CO_2 capture. Process simulations were performed by using the rate-based model in Aspen Plus. This work thoroughly analyzed and evaluated the industrial application performance of the MSC process, comparing it with conventional process and alternative modifications from other available research. Through careful analysis and integration of energy flows, a combined energy-optimized PCCC process was developed. Finally, strategies to improve the efficiency of the MSC process by parameter coupling regulation were proposed, along with the exploration of coupling other process modifications and utilizing alternative absorbents with a low regeneration duty. These efforts aim at reducing the energy requirements of CO_2 capture, which is critical for enhancing the feasibility and economics of carbon capture systems.

2. METHODOLOGY

Increasing the absorption cycling capacity, denoting the difference between rich and lean CO_2 loadings, is generally beneficial for reducing regeneration energy consumption.[33] This improvement results in a higher CO_2 capture per unit of absorbent, leading to a decrease in the absorbent flow rate. Simultaneously, higher CO_2 rich loading diminishes vapor partial pressure during the desorption process, thus reducing the regeneration energy.[34] However, as the CO_2 loading increases, the driving force for gas−liquid mass transfer weakens, posing challenges for escalating rich CO_2 loading within limited reaction space and time. Therefore, it is crucial to strive for the maximum theoretical CO_2-cycling capacity to reduce the regeneration energy requirement. Accordingly, an MSC process was proposed that distinctly separated various absorption stages, enabling flexible and decoupled management of operating parameters. The stages include the first stage of CO_2 efficient capture, the second stage of CO_2 absorption enhancement, and the third stage of CO_2-loading enrichment. By recycling the absorbent, the CO_2 absorption cycling capacity can be increased, thereby reducing the regeneration energy consumption.

2.1. MSC Process Description. The flue gas properties were derived from a carbon capture facility of 150,000 ton/year within a power plant.[35] The assumed flow rate of the flue gas was 100,000 N m^3/h. The composition of simulated flue gas entering the CO_2 absorption unit was assumed to be the actual flue gas after removal of SO_2 and NO_x by flue gas

https://doi.org/10.1021/acs.energyfuels.3c04115
Energy Fuels 2024, 38, 2129−2140

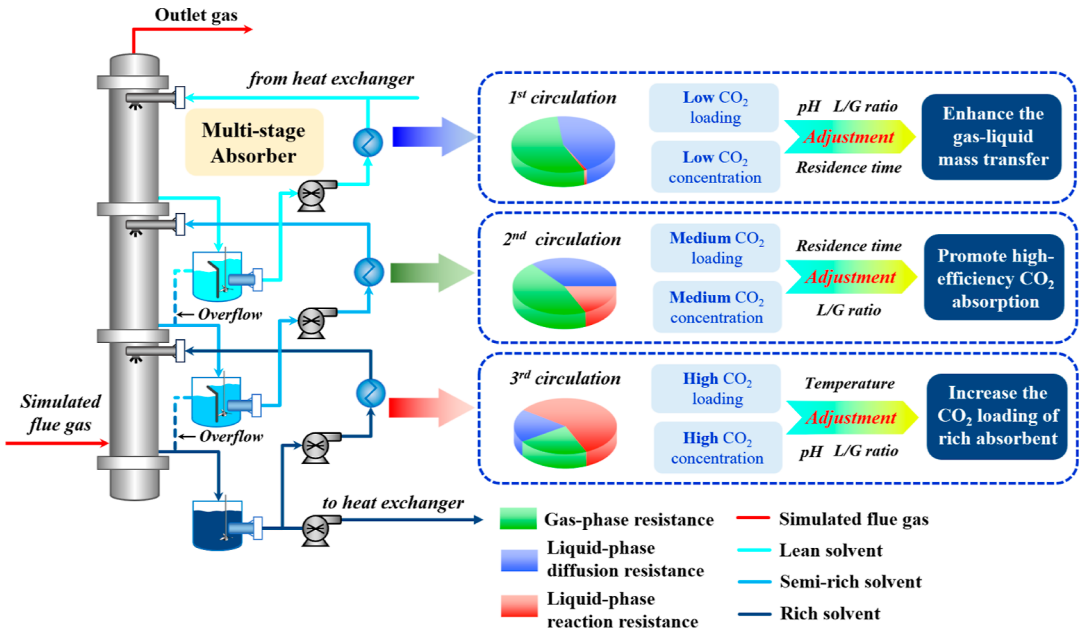

Figure 1. Schematic representation of MSC process.

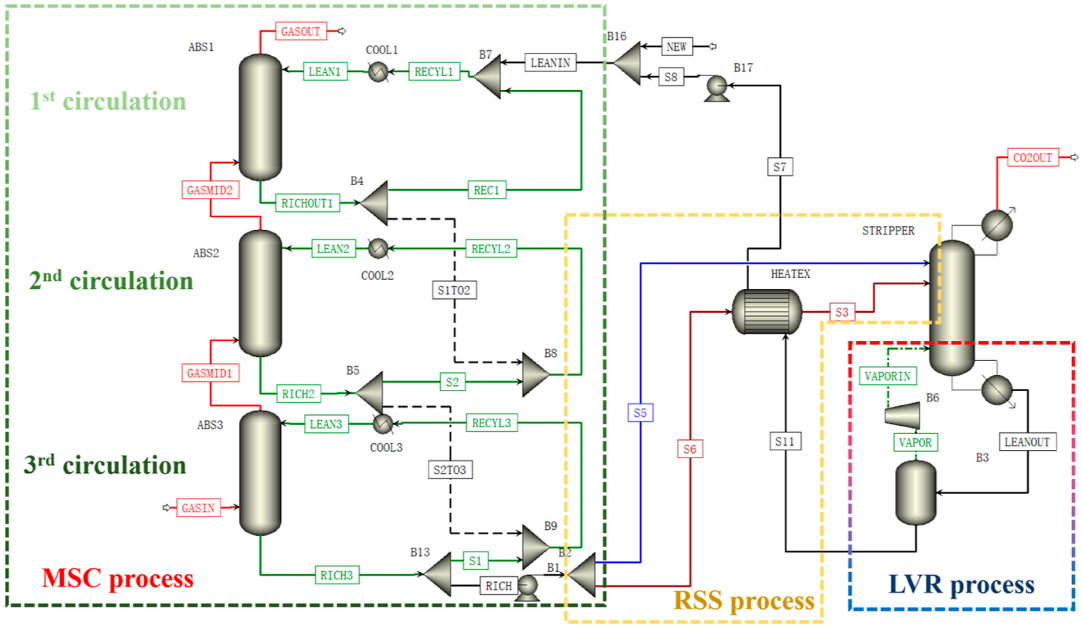

Figure 2. Scheme of the MSC process combined with RSS and LVR modifications in Aspen Plus.

desulfurization and selective catalytic reduction units, consisting of 70.7% N_2, 11.1% CO_2, 6.1% O_2, and 12.1% H_2O.

Figure 1 illustrates the schematic diagram of the MSC process. The lean solvent enters the top of the absorber of the first circulation absorber, along with the recirculated portion from the outlet of first circulation. At the outlet of each circulation, the rich solvent is divided into two segments: one overflows to the subsequent circulation, while the other, after cooling, is pumped back into the previous stage. The flue gas enters the bottom of the absorber, passes sequentially through the third, second, and first circulation, makes contact with the absorbent countercurrently, and finally exits the top of the absorber. Mass transfer resistance, comprising gas-phase resistance, liquid-phase diffusion resistance, and reaction resistance, is believed to vary at different absorber positions during the CO_2 absorption process.[36] The MSC process proposed includes several circulating pumps and tanks, which provide flexibility in controlling the absorption temperature, liquid−gas (L/G) ratio, and residence time. Enhancement of the CO_2 absorption efficiency is achieved by adjusting the L/G ratio and the residence time of the absorbent in contact with the flue gas during the circulation. Meanwhile, it is crucial to maintain a reduced pH level and low temperature in the third circulating tank to ensure comprehensive CO_2 enrichment. Notably, this work focuses on investigating the CO_2 absorption efficiency and energy consumption, excluding flue gas prescrubbing and the aerosol capture stage from consideration. The Aspen Plus simulation procedure is shown in Figure 2. To simplify the process modeling, the absorber is divided into thirds and arranged in series, although in practice, the three

https://doi.org/10.1021/acs.energyfuels.3c04115
Energy Fuels 2024, 38, 2129−2140

packings are continuously connected. The comparison between the conventional process and the MSC process is presented in Table 1.

Table 1. Comparison of Model Parameters between the Conventional Process and MSC Process

part	parameter	conventional process	MSC process
absorber	total column height, m	52	40
	column diameter, m	5	5
	L/G ratio[a], L/m^3	2.5−5.0	3.0−4.0
			4.5−6.0
			6.0−8.0
	CO_2 capture rate, %	90	90
	intercooling temperature, °C		50
heat exchanger	LMTD[b], °C	5	5
stripper	stripper column height, m	40	40
	stripper diameter, m	4	4

[a]L/G ratio—for MSC process, the values represent the L/G ratio of 1st, 2nd and 3rd stage, respectively. [b]LMTD—logarithmic mean temperature difference.

2.2. Chemical Reactions. The rate-based model, which is embedded in the Rad Frac model in Aspen Plus, was used to predict the CO_2 capture process. In contrast to the equilibrium model, the rate-based model provides a more precise reflection of the gas−liquid phase mass transfer rate within the column.[37] The CO_2 capture process was performed in Aspen Plus V12.0, employing the MDEA−PZ−CO_2−H_2O physical property package. The electrolyte non-random two liquid model, which is proven to be effective in predicting the properties between the liquid and gas phases, was utilized. In this study, the mixed flow model was chosen to calculate the heat and mass transfer during the process. The model uses the exit physical properties of each stage as the main physical properties of the gas−liquid phase with the liquid film being discretized. A geometrically modeled membrane discretization is utilized, which means that a consistent ratio of membrane thicknesses is maintained in the vicinity of the discretized regions. The membrane discretization ratio was set to the default value.

Tables 2 and 3 list the reactions involved in the combined PZ/MDEA−CO_2 capture process. Reactions 1−5 exhibit thermodynamic control due to their rapid reaction rates. The reaction equilibrium constant (K_{eq}) is expressed by eq 1. Reactions 6−13 are considered kinetically controlled due to their restricted reaction rates. The reaction rate constant (R) is expressed in eq 2.

Table 3. Kinetic Reaction Property in the Electrolyte PZ−MDEA−CO_2−H_2O System[24]

no.	type	reaction	k	E (J/mol)
6	kinetic	$CO_2 + OH^- \rightarrow HCO_3^-$	4.32×10^{13}	55407.32
7	kinetic	$HCO_3^- \rightarrow CO_2 + OH^-$	2.38×10^{17}	123164.1
8	kinetic	$PZ + CO_2 + H_2O \rightarrow PZCOO^- + H_3O^+$	4.14×10^{10}	33616.17
9	kinetic	$PZCOO^- + H_3O^+ \rightarrow PZ + CO_2 + H_2O$	7.94×10^{21}	65899.96
10	kinetic	$PZCOO^- + CO_2 + H_2O \rightarrow PZ(COO)_2^{2-} + H_3O^+$	3.62×10^{10}	33616.17
11	kinetic	$PZ(COO)_2^{2-} + H_3O^+ \rightarrow PZCOO^- + CO_2 + H_2O$	5.56×10^{25}	76831.70
12	kinetic	$MDEA + CO_2 + H_2O \rightarrow MDEAH^+ + HCO_3^-$	2.22×10^{7}	37759.28
13	kinetic	$MDEAH^+ + HCO_3^- \rightarrow MDEA + CO_2 + H_2O$	1.06×10^{16}	106323.2

$$\ln K_{eq} = A + B/(t + 273.15) + C \ln(t + 273.15) + D(t + 273.15) \quad (1)$$

$$R = k\, e^{-E/R(t+273.15)} \quad (2)$$

where T is for temperature, K; k is for pre-exponential factor; E is for activation energy, J/mol; R is for the universal gas constant, 8.314 J/mol/K.

2.3. Energy Calculations. The reboiler duty (Q_{reb}) consists of three components: CO_2 desorption reaction heat (Q_{rec}), solvent sensible heat (Q_{sen}), and vaporization heat (Q_{vap}) (eq 3).[38]

$$Q_{reb} = Q_{rec} + Q_{sen} + Q_{vap} \quad (3)$$

The reaction enthalpy (eq 4) corresponds to the heat of absorption of the amine with CO_2, which is in order to desorb CO_2 in the stripping process.[39] The sensible heat (eq 5) corresponds to the energy consumption of heating the rich solvent to the stripping temperature. The vaporization heat (eq 6) corresponds to the thermal loss of steam from the stripper and the energy needed to heat the refluxed water as it returns from the condenser to the stripper.

$$Q_{rec} = -n_{CO_2} \Delta H_{abs,CO_2} \quad (4)$$

$$Q_{sen} = m C_p (t_{reb} - t_{rich}) \quad (5)$$

$$Q_{vap} = n_{vap} \Delta H_{vap} + n_{cond} C_{p,H_2O} (t_{rich} - t_{cond}) \quad (6)$$

where n_{CO_2} is the flow rate of desorbed CO_2, kmol/h; $\Delta H_{abs,CO_2}$ is the reaction enthalpy of amine and CO_2, kJ/kmol; m is the flow rate of rich solvent, kg/h; C_p is the average specific heat capacity of rich solvent, kJ/(kg·°C); t_{reb} is the temperature of reboiler, °C; t_{rich} is the temperature of inlet rich solvent of the stripper, °C; n_{vap} is the flow rate of vapor escaping from the stripper to the condenser, kg/h; ΔH_{vap} is the

Table 2. Equilibrium Reaction Property in the Electrolyte PZ−MDEA−CO_2−H_2O System[24]

no.	type	reaction	A	B	C	D
1	equilibrium	$2H_2O \leftrightarrow H_3O^+ + OH^-$	132.9	−13446	−22.48	0
2	equilibrium	$HCO_3^- + H_2O \leftrightarrow CO_3^{2-} + H_3O^+$	216	−12432	−35.48	0
3	equilibrium	$PZH^+ + H_2O \leftrightarrow PZ + H_3O^+$	−4.0762	−7773.2	0	0
4	equilibrium	$H_2O + HPZCOO^- \leftrightarrow H_3O^+ + PZCOO^-$	−14.042	−3443.1	0	0
5	equilibrium	$MDEAH^+ + H_2O \leftrightarrow MDEA + H_3O^+$	−9.4165	−4234.98	0	0

https://doi.org/10.1021/acs.energyfuels.3c04115
Energy Fuels 2024, 38, 2129−2140

vaporization heat of H_2O, kJ/kg; n_{cond} is the flow rate of refluxed water, kg/h; C_{p,H_2O} is the heat capacity of H_2O, kJ/(kg·°C); t_{cond} is the temperature of refluxed water, °C.

The total energy consumption of the CO_2 capture process consists of four primary components: absorber regeneration heat (W_{reg}), CO_2 compression work (W_{comp}), pump work (W_{pump}), and recompression work (W_{recomp}). The equation of total equivalent work is provided by eq 7.[40] Compared to the conventional process, the proposed MSC process added additional pump work for recirculating the solvent from the overflow tanks back to the inlet of each stage along with pumping to recirculate the intercooling water. Notably, the pump work also included the energy required to elevate the pressure of the rich solvent from absorption pressure to desorption pressure, applicable to both the conventional and the MSC processes. The recompression work was exclusively considered in the LVR process. Both pump and compressor work were directly derived from Aspen Plus, with the pump efficiency assumed to be 72%.

$$W = W_{reg} + W_{comp} + W_{pump} + W_{recomp} \tag{7}$$

The equivalent electricity of reboiler duty (W_{reg}) is expressed by eq 8.[41]

$$W_{reg} = Q_{reb}\eta\left(\frac{t_{reb} + \Delta t - t_{sink}}{t_{reb} + 273.15 + \Delta t}\right) \tag{8}$$

where the Q_{reb} is the reboiler duty, GJ/t CO_2; η is the turbine efficiency, while is assumed to be 90% in this study; Δt is assumed to be 5 °C; t_{sink} is assumed to be 50 °C.

The compression work is calculated by eq 9.[42]

$$W_{comp} = 4.572 \ln\left(\frac{150}{P_s}\right) - 4.096 (P_s \leq 4.56 \text{ bar}) \tag{9}$$

where P_s is the stripping pressure, bar.

2.4. Model Validation. In our previous work,[43] we have used a small-scale MSC experimental platform to investigate and evaluate the absorption performance and regeneration duty of the MSC process.[44] Simultaneously, the MSC process was modeled and studied by using Aspen Plus. As shown in Figure 3, the simulation results were all within the error bars of the experimental data, confirming the reliability of the model. The minor errors are possibly due to fluctuations in the rich solvent flow rate and reboiler temperature during the experiment. The simulation of the conventional process with the base case configuration was modeled and validated against publicly available pilot experiment data as well as simulation results from various researchers, encompassing both MEA and PZ/MDEA. As shown in Table 4, the simulation results of regeneration energy in this work were within a reasonable range compared to the published data. These results indicated the effectiveness of the model in predicting the performance of the MSC process. The deviation may be due to several factors: CO_2 concentration of flue gas; scale of the capture process; stripping pressure; column parameters; different modifications. It is also worth noting that unlike the simulation, the CO_2 loading of the lean solvent experiences continuous fluctuations during the pilot experiment. The variation of the CO_2 lean loading will bring a deviation of regeneration energy (refer to Section 3.3.1). The challenges of maintaining a steady state during real experimental manipulations should not be overlooked.

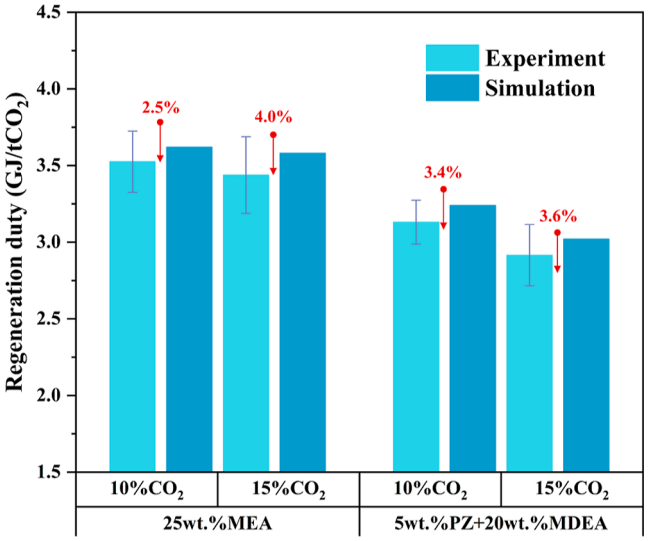

Figure 3. Comparison of experiment and simulation results of the CO_2 regeneration duty.

3. RESULTS AND DISCUSSION

In this section, the CO_2-loading variations at each stage of the MSC process were analyzed, and the performance of the MSC process was assessed in comparison to both the conventional process and the AIC process. Sensitivity analyses were performed for key parameters, including the PZ/MDEA ratio, CO_2 capture rate, intercooling temperature, CO_2 lean loading, and stripping temperature. Furthermore, based on the MSC process, the RSS and LVR modifications were integrated to achieve a minimized regeneration duty.

3.1. Analysis and Evaluation of MSC Process. Simply increasing the solvent flow rate to achieve the target capture rate is impractical due to the resulting elevated sensible heat. The MSC process integrates the advantages of both the AIC and RSR processes, increasing the L/G ratio in various parts of the absorber, while keeping the stripper flow rate unchanged. Figure 4 illustrates the CO_2 absorption proportion and outlet CO_2 loading for each circulation. The employed absorbent consists of 5 wt % PZ and 45 wt % MDEA, with a CO_2 lean loading set at 0.04. Observably, the first and second circulations exhibited a higher proportion of CO_2 absorption, while less proportion of CO_2 was absorbed during the third stage. The CO_2 loading of the absorbent gradually increases as the stage proceeds. Table 5 compares the conventional process, AIC process, and MSC process. It is considered that the MSC process requires additional pumping work for recirculation. The MSC process achieved a notable reduction in reboiler duty from 2.97 GJ/t CO_2 to 2.51 GJ/t CO_2, a reduction of 15.5% compared to the conventional process. Additionally, the total equivalent work decreased by 9.6%, from 0.251 MW h/t of CO_2 to 0.227 MW h/t CO_2. Compared to the AIC process, the MSC process still exhibited a 5.3% decrease in reboiler duty and a 3.0% reduction in total equivalent work, highlighting its better performance.

3.2. Performance Analysis of Absorption Process. *3.2.1. Effect of PZ/MDEA Ratio.* Simulation results and available research findings[24,25] both indicated that an optimal CO_2 lean loading corresponds to each specific PZ/MDEA ratio, thereby achieving the minimum reboiler duty. Figure 5 illustrates the impacts of the PZ/MDEA ratio on the CO_2 cycling capacity, heat duties, and total equivalent work. For

https://doi.org/10.1021/acs.energyfuels.3c04115
Energy Fuels 2024, 38, 2129−2140

Table 4. Contrasting with Prior Research Conducted Based on PZ/MDEA and MEA

	PZ + MDEA				MEA		
	this work	Zhao[24]	Mostafavi[29]	this study	Li[28]	Liu[32]	Ayittey[45]
CO_2 concentration, %	**11.1**	12	8.8	11.1	11.9	12.8	11.1
flue gas temperature, °C	**50**	41	52	50	50	53.7	57.9
CO_2 capture rate, %	**90**	90	90	90	85	90	86
absorber pressure, MPa	**1**	1.2	1.1	1	1.06	1	1
absorbent concentration, %	**5/45**	20/30	12.5/30	30	35	30	28.5
stripping pressure, MPa	**2.1**	2.2	1.5	2.1	2	1.8	2
regeneration duty, GJ/t CO_2	**2.97**	2.74	2.9	3.64	3.6	3.85	3.98
deviation, %		7.7	2.4		1.1	5.8	9.3

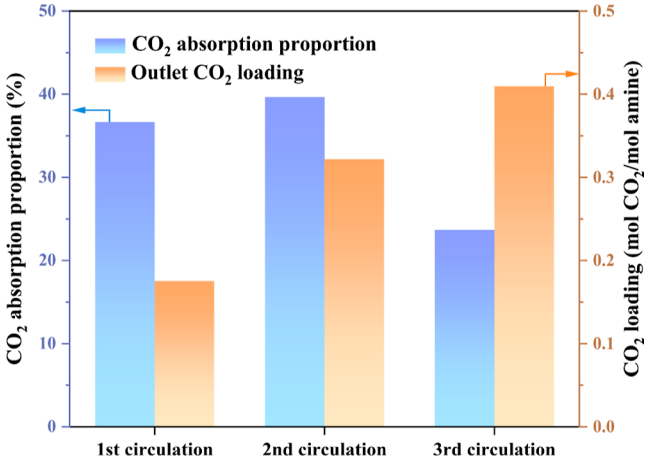

Figure 4. Outlet CO_2 loadings and the CO_2 absorption proportion at each stage of the MSC process.

Table 5. Comparison of the Performance Including the Conventional Process, the AIC Process, and the MSC Process

	conventional process	AIC process	MSC process
absorbent solutions	5 wt % PZ + 45 wt % MDEA		
CO_2 lean loading, mol/mol	0.04	0.04	0.04
inlet solvent flow, t/h	381.0	327.3	235.5
L/G ratio, L/m^3	3.45	2.79	4.0/5.0/7.0[a]
CO_2 capture rate, %	90	90	90
intercooling temperature, °C		50	50
flow of rich solvent, t/h	392.5	342.4	252.6
stripper pressure, MPa	0.20	0.20	0.20
	Simulation Result		
CO_2-cycling capacity, mol/mol	0.26	0.35	0.38
reboiler duty, GJ/t CO_2	2.97	2.65	2.51
equivalent work, MW h/t CO_2	0.251	0.234	0.227

[a]The L/G ratios of 1st to 3rd circulation were set to 4.0, 5.0, and 7.0, respectively.

each ratio, the minimum reboiler duty and the corresponding CO_2 lean loading were selected. The stripping pressure was uniformly set to 0.20 MPa. As shown in Figure 5a, as the PZ/MDEA ratio adjusted from 5/45 wt % to 20/30 wt %, the CO_2 lean loading associated with the minimum regeneration duty increased from 0.04 to 0.11 mol CO_2/mol amine, aligning with previous literature results.[46] Figure 5b demonstrates that the reduced rich solvent flow rate led to a decrease of sensible heat, while the increased CO_2 rich loading resulted in a simultaneous reduction of vaporization heat. However, the reaction heat increased due to the higher enthalpy (86 kJ/mol CO_2) of PZ compared to the MDEA (58 kJ/mol CO_2).[22,47] The minimum reboiler duty of 2.503 GJ/t CO_2 and total equivalent work of 0.227 MW h/t CO_2 were attained with a 5 wt % PZ/45 wt % MDEA solution. It is worth noting that a relatively lower PZ content also reduced the volatilization loss. However, the reduction in absorption efficiency due to decreased PZ concentration should be carefully considered in practical applications.

3.2.2. Effect of CO_2 Capture Rate. The regeneration energy consumption would be directly influenced by the rate of CO_2 capture rate. Figure 6 illustrates the impact of CO_2 capture rate on reboiler duty, rich solvent flow rate and CO_2 rich loading. At a PZ/MDEA ratio of 5/45 wt % and a CO_2 rich loading of 0.04, the reboiler duty reduced by 2.2% when the CO_2 capture rate decreased from 95 to 90%, and by 2.1% when the it further decreased from 90 to 80%. At low CO_2 partial pressure, the larger mass transfer resistance makes it more difficult to absorb CO_2. Therefore, as the CO_2 capture rate increases, the CO_2 rich loading decreases, resulting in a higher reboiler duty. While increasing the CO_2 capture rate from 90 to 95% may incur additional costs of CO_2 capture, 90% is generally considered to be the industry standard. In this study, the 90% capture rate was used to evaluate the performance of the MSC process in an industrial configuration.

3.2.3. Effect of Intercooling Temperature. Since the CO_2 absorption by amines is an exothermic process, it will elevate the internal temperature of the absorber, leading to a contrary shift in the absorption equilibrium. Consequently, the CO_2 loading of rich solvent and cycling capacity were constrained. To address this issue, intercoolers were positioned at the inlet of each stage in order to lower the internal temperature of the absorber column. This caused the reaction to proceed in a positive direction, leading to an increase in the CO_2 rich loading, which is considered favorable for reducing the reboiler duty. However, the decrease in the intercooling temperature also lowered the temperature of the rich solvent, which necessitated additional sensible heat to be consumed. Notably, the cost of circulating the cooling water also increased. Figure 7 demonstrates that reducing the intercooling temperature from 55 to 40 °C resulted in a decrease in reboiler duty from 2.53 GJ/t CO_2 to 2.46 GJ/t CO_2. Considering the practicality of actual industrial equipment, an intercooling temperature of 50 °C was chosen for this study.

3.3. Performance Analysis of Stripping Process. *3.3.1. Effects of CO_2 Lean Loading.* The CO_2 lean loading indicates the extent to which the stripper completely removes CO_2, and it will significantly influence the regeneration duty.

https://doi.org/10.1021/acs.energyfuels.3c04115
Energy Fuels 2024, 38, 2129−2140

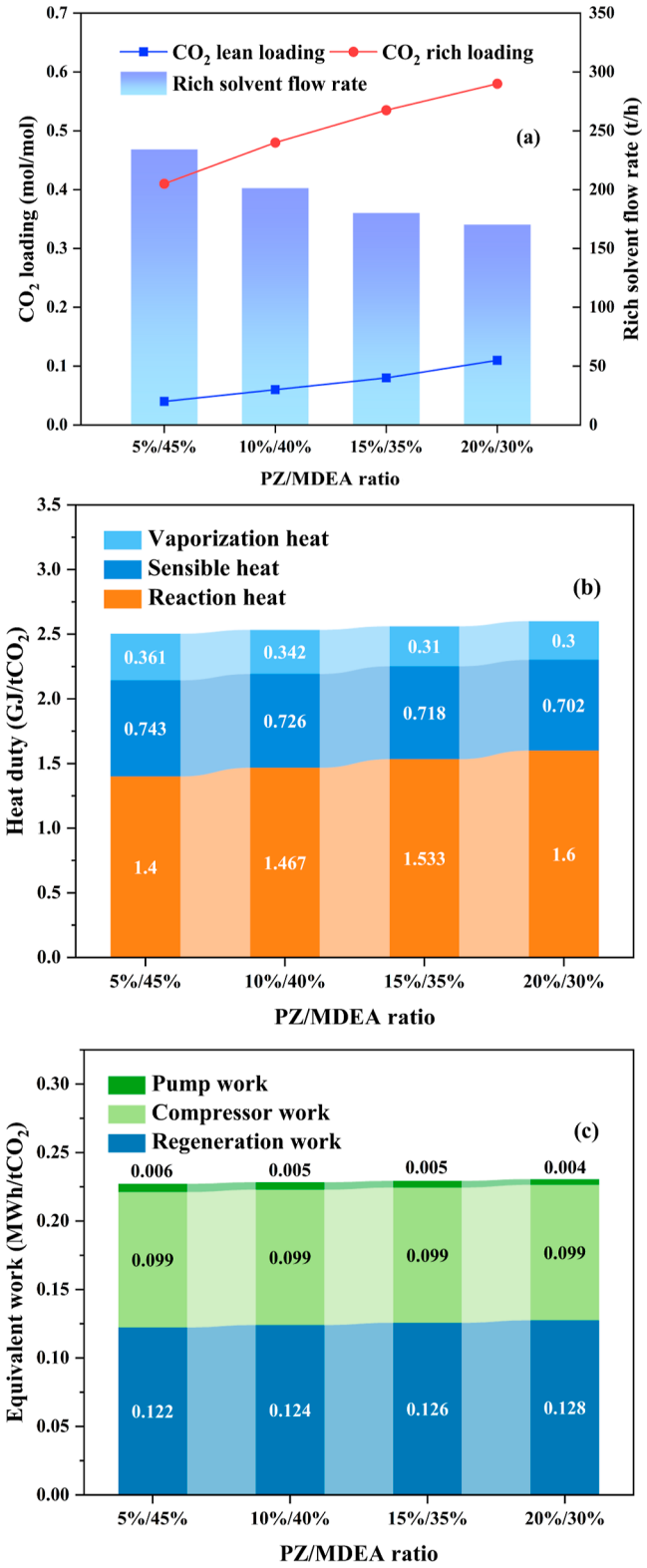

Figure 5. Effect of PZ/MDEA ratio on (a) CO_2 loading and flow rate of rich solvent, (b) total regeneration duty and heat duties; (c) total equivalent work.

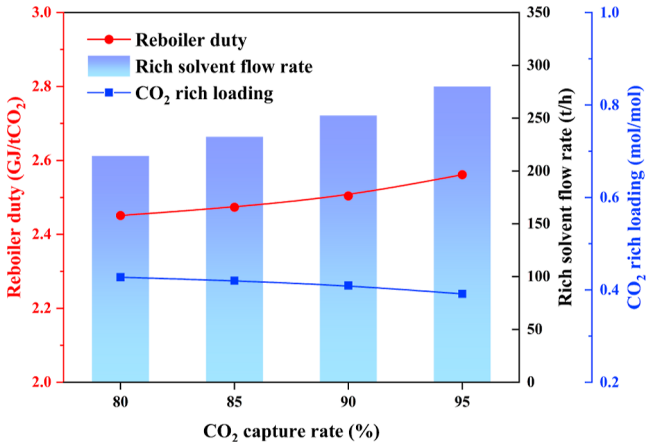

Figure 6. Effect of CO_2 capture rate on reboiler duty, flow rate of rich solvent and CO_2 loading of rich solvent.

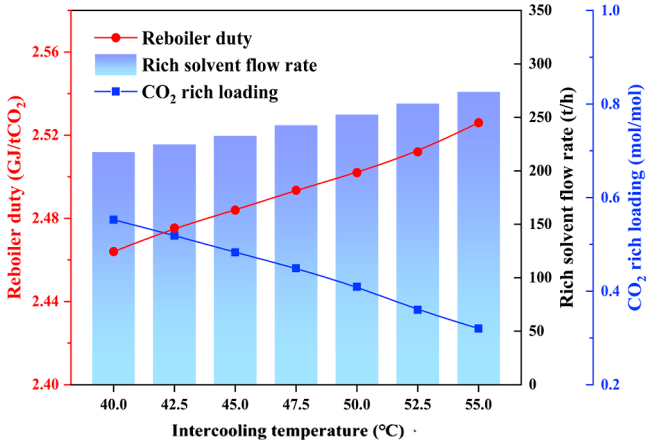

Figure 7. Effect of solvent temperature on reboiler duty, flow rate of rich solvent, and CO_2 loading of rich solvent.

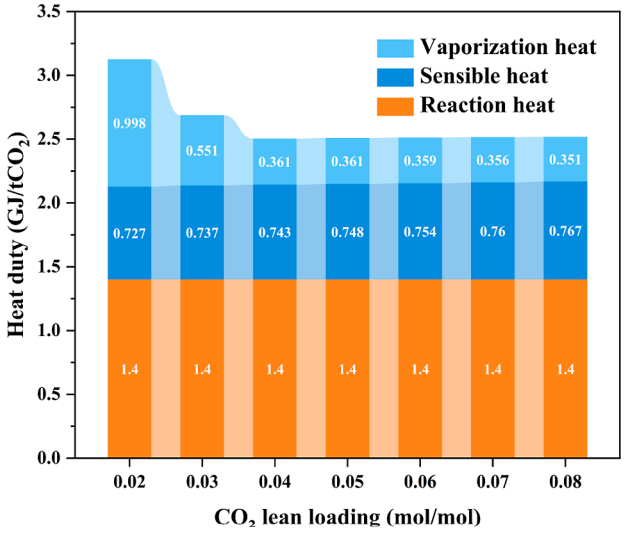

Figure 8. Effect of CO_2 loading of lean solvent on regeneration duty (5 wt % PZ/45 wt % MDEA, stripping pressure = 0.20 MPa).

As shown in Figure 8, as the CO_2 lean loading increases, the reboiler duty first decreases and then increases. Under specific solutions and conditions, the reaction heat and the CO_2 rich loading remained constant. Consequently, an increase in flow rate led to a rise in sensible heat. However, elevating the CO_2 lean loading reduced the need for exhaustive desorption and subsequently lowering the vaporization heat.[48] Therefore, a trade-off existed between the sensible heat and the vaporization heat. Insufficient CO_2 lean loading led to a significant

https://doi.org/10.1021/acs.energyfuels.3c04115
Energy Fuels 2024, 38, 2129−2140

increase in the vaporization heat, resulting in a higher total regeneration energy. Conversely, excessive CO_2 lean loading led to an increase in sensible heat that outweighed the reduction in vaporization heat, resulting in a slight increase in the regeneration energy. Thus, there was an optimal lean load range that minimized the regeneration duty. For 5 wt % PZ/45 wt % MDEA, the minimum required regeneration energy was obtained at 0.04 mol CO_2/mol amine, approximately 2.503 GJ/t CO_2.

3.3.2. Effects of Stripping Pressure. Figure 9 illustrates the effect of stripping pressure on heat duties and equivalent works. In general, a lower pressure promotes CO_2 desorption. However, increasing the stripping pressure reduced the vapor proportion of regeneration gas, leading to a reduction in vaporization.[34] Meanwhile, the elevated stripping pressure raised the temperature of the outlet lean solvent, resulting in an increase in the sensible heat. As shown in Figure 9a, the optimum regeneration energy occurred at a stripping pressure of 0.13 MPa. Figure 9b reveals that a higher stripping pressure reduced the subsequent CO_2 compression work while simultaneously increasing the regeneration work due to the elevated temperature. Therefore, the total equivalent work initially decreased but then increased as the stripping pressure rose. Remarkably, although the variation in the total equivalent work was very small, the opposite variations between the regeneration work and the compression work should not be ignored.

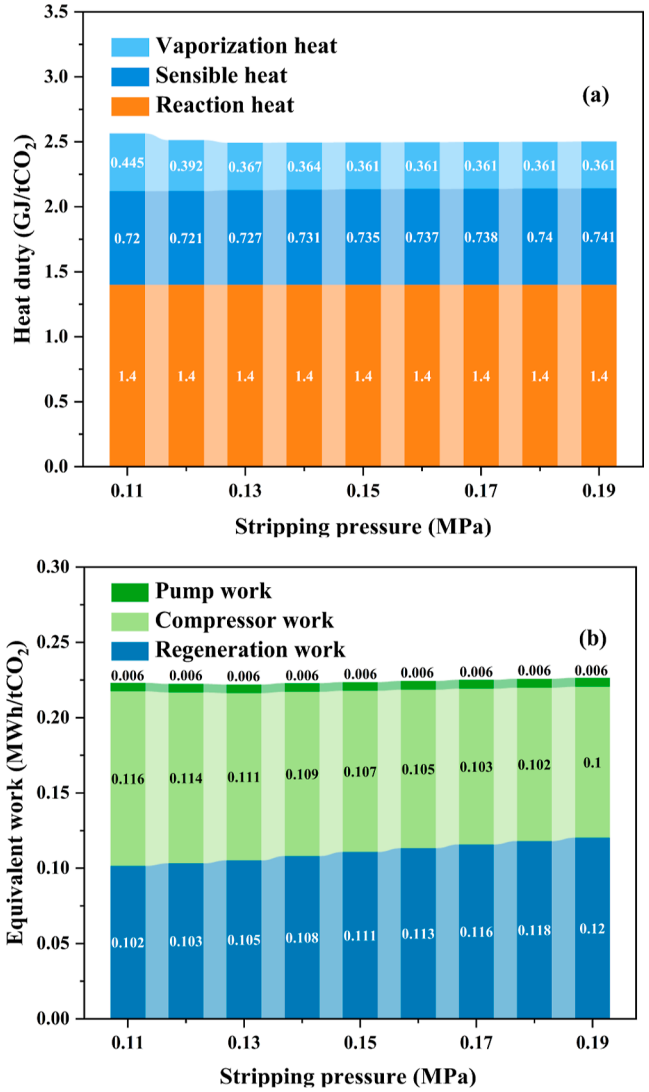

Figure 9. Effects of stripping pressure on (a) heat duties; (b) equivalent work (5 wt % PZ/45 wt % MDEA, CO_2 lean loading = 0.04).

3.4. Process Modification. *3.4.1. RSS Modification.* The RSS modification involved directing a portion of the rich solvent to the top position of the stripper while another portion entered the middle position after heat exchange. The latter, hot-rich solvent was first heated to produce regeneration gas. Meanwhile, the cold-rich solvent, introduced at the upper part, recovered heat from high-temperature regenerated gas to facilitate the desorption of CO_2. As demonstrated in Figure 10a, the reboiler duty was affected by the split fraction with the optimal fraction identified as 0.20. Notably, the temperature of the lean solvent at the reboiler outlet remained constant regardless of changes in the split fraction. Therefore, the RSS modification reduced the vaporization heat while simultaneously introducing sensible heat. An optimal split fraction of 0.20 resulted in a reduction of the reboiler duty from 2.49 GJ/t CO_2 to 2.30 GJ/t CO_2, a reduction of 7.6% compared to

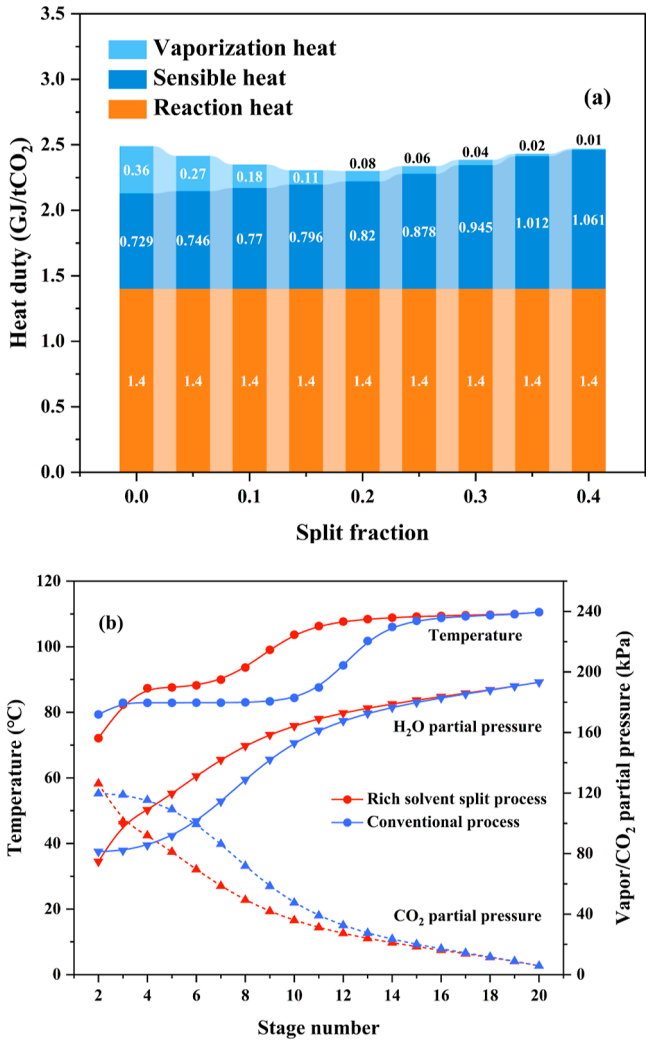

Figure 10. (a) Effects of RSS fraction on regeneration duty; (b) temperature and vapor/CO_2 partial pressure along the stripper.

https://doi.org/10.1021/acs.energyfuels.3c04115
Energy Fuels 2024, 38, 2129−2140

nonsplitting. As shown in Figure 10b, the RSS modification elevated the temperature gradient along the stripper. The temperature decreased at the upper part due to entry of the cold-rich solvent. Meanwhile, the middle section of the stripper experienced a higher temperature of the liquid phase in most stages, which promoted the desorption of CO_2. This heightened CO_2 partial pressure and reduced H_2O partial pressure at the stripper outlet contributed to preferable CO_2 desorption.

3.4.2. LVR Modification. The LVR modification incorporated a flash tank to evaporate the high-temperature lean solvent from the reboiler. The steam produced in the flash tank was recompressed by a compressor and reintroduced into the stripper, facilitating the recovery of heat from the flash steam of the lean solvent. This modification effectively reduced the reboiler duty associated with the stripping process. As illustrated in Table 6, the integration of the LVR modification within the MSC process yielded a noteworthy reduction of 7.2% in the reboiler duty. Although the LVR modification required additional compressor power consumption and entailed an increase in the compression work, it still resulted in a commendable 2.3% reduction in the total equivalent work.

Table 6. Comparison of the Performance of Only with MSC Process and Combined MSC and LVR Process

	MSC process	MSC & LVR process	deviation, %
CO_2 lean loading, mol/mol	0.04	0.04	
stripping pressure, MPa	0.13	0.13	
flash pressure, MPa		0.1	
reboiler duty, GJ/t CO_2	2.49	2.31	7.2
equivalent regeneration work, MW h/t CO_2	0.105	0.097	18.0
compression work, MW h/t CO_2	0.111	0.114	−15.2
pump work, MW h/t CO_2	0.006	0.006	0
total equivalent work, MW h/t CO_2	0.222	0.217	2.3

3.4.3. Combined Process. The combined process integrated the RSS and LVR processes into the MSC process framework. As demonstrated in Table 7, compared to the conventional process, the combined process reduced the reboiler duty from 2.99 GJ/t CO_2 to 2.16 GJ/t CO_2, representing a substantial reduction of 27.8%, and decreased the total equivalent work from 0.238 MW h/t CO_2 to 0.211 MW h/t CO_2, with a reduction of 11.3%. The regeneration duty of the MSC-based combined process was compared with the existing field and simulation results of available researches in Table 8. The MSC-based combined process achieved a remarkably low regeneration energy consumption of 2.16 GJ/t of CO_2, indicating widespread potential for MSC process application.

3.5. Discussion on Improving the CO_2 Capture Performance by Using the MSC Process. In practical application scenarios, the parameters of flue gas are generally complex and unstable, which may negatively affect the CO_2-removal efficiency, regeneration energy consumption, and stability of the PCCC process. To overcome these challenges, various flexible and decoupled regulation methods have been proposed for optimizing parameters such as temperature, L/G ratio, pH, and residence time. Moreover, except for MSC process, the potential for coupling other process modifications and the utilization of alternative absorbents with low regeneration energy is discussed.

Table 7. Comparison of the Specific Configurations and Performance Including the Conventional Process, Only with the MSC Process and the Combined Modifications Process

	conventional process	MSC process	combined process (MSC + RSS + LVR)
absorbent solutions	5 wt % PZ + 45 wt % MDEA		
CO_2 lean loading, mol/mol	0.04	0.04	0.04
inlet solvent flow, t/h	381.0	235.5	235.5
CO_2 capture proportion, %	90	90	90
intercooling temperature, °C		50	50
flow of rich solvent, t/h	392.5	252.6	252.6
stripper pressure, MPa	0.13	0.13	0.13
rich split fraction, %			20
flash pressure, MPa			0.1
	Simulation Result		
CO_2 rich loading, mol/mol	0.30	0.42	0.42
CO_2-cycling capacity, mol/mol	0.26	0.38	0.38
reboiler duty, GJ/t CO_2	2.99	2.49	2.16
equivalent regeneration work, MW h/t CO_2	0.126	0.105	0.091
compression work, MW h/t CO_2	0.111	0.111	0.114
pump work, MW h/t CO_2	0.001	0.006	0.006
total equivalent work, MW h/t CO_2	0.238	0.222	0.211

From Section 3.1, the first and second stages are the primary CO_2 absorption parts of the MSC process. The final stage, on the other hand, contributes to only a small proportion of the CO_2 absorption and serves mainly to enhance the CO_2 loading of the rich solvent. At the primary absorption stage, the regenerated fresh solvent tends to absorb CO_2 easily in an exothermic reaction, so efficient CO_2 capture can be achieved by increasing the local L/G ratio and lowering the reaction temperature. At the CO_2 enrichment stage, as the reaction progresses, the gradual increase in CO_2 loading leads to a decrease in the solution pH and the CO_2 absorption rate. Optimal CO_2 enrichment is attained by extending the reaction residence time of the amine and adjusting the L/G ratio.

From Section 3.3, coupling other modifications within the MSC process framework can further reduce regeneration energy consumption. The modifications aim to recover the heat provided by reboiler during the stripping process. For example, the RSS modification is used to recover heat from the stripped gas at the top of the stripper, and the LVR modification is employed to recover the heat from the lean solvent. Additional comparable modifications include rich solvent preheating,[45] stripper interheating[52] and parallel exchanger arrangement.[29] In practical large-scale CO_2 capture processes, combining the MSC process with various heat recovery and reuse modifications presents an opportunity to break through the bottleneck of high energy consumption.

The performance of the MEA absorbent in the MSC process was also investigated in this work, revealing a reduction in regeneration duty from 3.60 GJ/t CO_2 to 3.51 GJ/t CO_2, amounting to only 2.5% compared to the conventional process.

https://doi.org/10.1021/acs.energyfuels.3c04115
Energy Fuels 2024, 38, 2129−2140

Table 8. Comparison of Regeneration Energy Consumption of this Work and Other Works

absorbent	regeneration duty, GJ/t CO_2	flue gas CO_2 concentration, %	modifications	reference
		Field Data		
30.3% MEA	3.98	16.5		49
32.3% MEA	3.86	11.9		28
		Simulation Data		
35% MEA	3.11	11.9	AIC, rich-split and stripper interheating	28
30% MEA	2.93	11.1	RSS, LVR and intercooling	35
40% DEA	3.40	14.6		50
5% DEA/25% AMP	3.03	13.3	gas precooling	51
12.5% PZ/30% MDEA	2.54	8.8	AIC, LVR and parallel exchanger arrangement	29
20% PZ/30% MDEA	2.24	12.0	AIC, RSS, stripper interheating and parallel exchanger arrangement	24
15% PZ/35% MDEA	2.44	12.0	RSS and rich vapor compression	25
5% **PZ/45%** MDEA	**2.16**	**11.1**	**MSC, RSS and LVR**	**this work**

Conversely, the regeneration energy consumption of PZ/MDEA in the MSC process was remarkably lower than MEA. Consequently, the MSC process is more suitable for MDEA-based absorbents, as it enhances the absorption efficiency and highlights the advantage of their low reaction heat. Meanwhile, increasing the CO_2 rich loading by the MSC process is conducive to reduce the sensible and latent heat. Moreover, the MSC process shows promise for the application of novel absorbents requiring low energy for regeneration, such as ionic liquids and biphasic solvents.

4. CONCLUSIONS

This work introduced an innovative MSC process designed to enhance CO_2 absorption and reduce the regeneration energy. A comprehensive simulation using Aspen Plus was performed to evaluate the MSC process compared to the conventional process. The results indicate that the MSC process was beneficial to enhance CO_2 absorption efficiency, increase cycling capacity, and reduce regeneration energy consumption. Compared to the conventional process, the MSC process achieved a 46.2% increase in cycling capacity and a 15.5% reduction in reboiler duty under the optimal conditions of 5 wt % PZ/45 wt % MDEA and 0.04 mol/mol lean solvent CO_2 loading. Moreover, the incorporation of RSS and LVR modifications within the MSC framework further reduced the reboiler duty and total equivalent work to 2.16 GJ/t of CO_2 and 0.211 MW h/t of CO_2, respectively. This represented a substantial reduction of 27.8 and 11.3%, respectively, compared to the conventional process. Finally, strategies to enhance the efficiency of the MSC process through parameter coupling regulation were proposed, along with a discussion on the potential for coupling other process modifications and utilizing alternative absorbents with low regeneration energy. This study aimed to provide a novel method for designing carbon capture system, offering important implications for achieving competitive carbon reduction.

AUTHOR INFORMATION

Corresponding Author

Chenghang Zheng − *State Key Lab of Clean Energy Utilization, State Environmental Protection Engineering Center for Coal-Fired Air Pollution Control, Zhejiang University, Hangzhou 310027, PR China; Zhejiang Laboratory of Energy and Carbon Neutralization, Hangzhou 310027, PR China;* orcid.org/0000-0003-0410-2007; Phone: +86-571-87951335; Email: zhengch2003@zju.edu.cn; Fax: +86-571-87951335

Authors

Chengjin Pan − *State Key Lab of Clean Energy Utilization, State Environmental Protection Engineering Center for Coal-Fired Air Pollution Control, Zhejiang University, Hangzhou 310027, PR China*

Chang Liu − *State Key Lab of Clean Energy Utilization, State Environmental Protection Engineering Center for Coal-Fired Air Pollution Control, Zhejiang University, Hangzhou 310027, PR China*

Lingyu Shao − *State Key Lab of Clean Energy Utilization, State Environmental Protection Engineering Center for Coal-Fired Air Pollution Control, Zhejiang University, Hangzhou 310027, PR China*

Feng Xu − *State Key Lab of Clean Energy Utilization, State Environmental Protection Engineering Center for Coal-Fired Air Pollution Control, Zhejiang University, Hangzhou 310027, PR China*

Zhicheng Wu − *State Key Lab of Clean Energy Utilization, State Environmental Protection Engineering Center for Coal-Fired Air Pollution Control, Zhejiang University, Hangzhou 310027, PR China*

Zhengang Zhou − *State Key Lab of Clean Energy Utilization, State Environmental Protection Engineering Center for Coal-Fired Air Pollution Control, Zhejiang University, Hangzhou 310027, PR China*

Xiao Zhang − *State Key Lab of Clean Energy Utilization, State Environmental Protection Engineering Center for Coal-Fired Air Pollution Control, Zhejiang University, Hangzhou 310027, PR China; Zhejiang Laboratory of Energy and Carbon Neutralization, Hangzhou 310027, PR China;* orcid.org/0000-0002-0342-3282

Yang Zhang − *Huadian Electric Power Research Institute Co., Ltd., Hangzhou 310030, PR China*

Xiang Gao − *State Key Lab of Clean Energy Utilization, State Environmental Protection Engineering Center for Coal-Fired Air Pollution Control, Zhejiang University, Hangzhou 310027, PR China; Zhejiang Laboratory of Energy and Carbon Neutralization, Hangzhou 310027, PR China; Jiaxing Research Institute, Zhejiang University, Jiaxing 314000, PR China;* orcid.org/0000-0002-1732-2132

Complete contact information is available at: https://pubs.acs.org/10.1021/acs.energyfuels.3c04115

https://doi.org/10.1021/acs.energyfuels.3c04115
Energy Fuels 2024, 38, 2129−2140

Notes

The authors declare no competing financial interest.

■ ACKNOWLEDGMENTS

This work was supported by the National Key Research and Development Program of China (no. 2022YFC3701500), Zhejiang Provincial Natural Science Foundation of China under grant (no. LDT23E0601), National Natural Science Foundation of China (no. 42341208) and the Key R&D Program of Zhejiang Province (no. 2023C03008).

■ REFERENCES

(1) Rogelj, J.; den Elzen, M.; Höhne, N.; Fransen, T.; Fekete, H.; Winkler, H.; Schaeffer, R.; Sha, F.; Riahi, K.; Meinshausen, M. Paris Agreement climate proposals need a boost to keep warming well below 2 °C. *Nature* **2016**, *534*, 631−639.

(2) Pan, S.-Y.; Chiang, P.-C.; Pan, W.; Kim, H. Advances in state-of-art valorization technologies for captured CO_2 toward sustainable carbon cycle. *Crit. Rev. Environ. Sci. Technol.* **2018**, *48*, 471−534.

(3) Sun, Q.; Xiong, J.; Gao, H.; Olson, W.; Liang, Z. Energy-efficient regeneration of amine-based solvent with environmentally friendly ionic liquid catalysts for CO_2 capture. *Chem. Eng. Sci.* **2024**, *283*, 119380.

(4) Goto, K.; Yogo, K.; Higashii, T. A review of efficiency penalty in a coal-fired power plant with post-combustion CO_2 capture. *Appl. Energy* **2013**, *111*, 710−720.

(5) Wang, Y.; Tian, Y.; Pan, S. Y.; Snyder, S. W. Catalytic processes to accelerate decarbonization in a net-zero carbon world. *ChemSusChem* **2022**, *15*, No. e202201290.

(6) Zhang, R.; Liu, R.; Barzagli, F.; Sanku, M. G.; Li, C.; Xiao, M. CO_2 absorption in blended amine solvent: speciation, equilibrium solubility and excessive property. *Chem. Eng. J.* **2023**, *466*, 143279.

(7) Zhang, R.; Liu, H.; Liu, R.; Niu, Y.; Yang, L.; Barzagli, F.; Li, C. . e.; Xiao, M. Speciation and gas-liquid equilibrium study of CO_2 absorption in aqueous MEA-DEEA blends. *Gas Sci. Eng.* **2023**, *119*, 205135.

(8) Gao, G.; Xu, B.; Gao, X.; Jiang, W.; Zhao, Z.; Li, X.; Luo, C.; Wu, F.; Zhang, L. New insights into the structure-activity relationship for CO_2 capture by tertiary amines from the experimental and quantum chemical calculation perspectives. *Chem. Eng. J.* **2023**, *473*, 145277.

(9) Zhang, X.; Zhang, S.; Tan, Z.; Zhao, S.; Peng, Y.; Xiang, C.; Zhao, W.; Zhang, R. One-step synthesis of efficient manganese-based oxide catalyst for ultra-rapid CO_2 absorption in MDEA solutions. *Chem. Eng. J.* **2023**, *465*, 142878.

(10) Yuan, C.; Wang, Y.; Baena-Moreno, F. M.; Pan, Z.; Zhang, R.; Zhou, H.; Zhang, Z. Review and perspectives of CO_2 absorption by water- and amine-based nanofluids. *Energy Fuels* **2023**, *37*, 8883−8901.

(11) Liu, B.; Wang, T.; Yang, X.; Chiang, P.-C. Experimental study on energy consumption and performance of hydroxyethyl ethylenediamine solution for CO_2 capture. *Aerosol Air Qual. Res.* **2019**, *9*, 2929−2940.

(12) Gao, W.; Liang, S.; Wang, R.; Jiang, Q.; Zhang, Y.; Zheng, Q.; Xie, B.; Toe, C. Y.; Zhu, X.; Wang, J.; Huang, L.; Gao, Y.; Wang, Z.; Jo, C.; Wang, Q.; Wang, L.; Liu, Y.; Louis, B.; Scott, J.; Roger, A.-C.; Amal, R.; He, H.; Park, S.-E. Industrial carbon dioxide capture and utilization: state of the art and future challenges. *Chem. Soc. Rev.* **2020**, *49*, 8584−8686.

(13) Kim, I.; Svendsen, H. F. Heat of absorption of carbon dioxide (CO_2) in monoethanolamine (MEA) and 2-(aminoethyl)-ethanolamine (AEEA) solutions. *Ind. Eng. Chem. Res.* **2007**, *46*, 5803−5809.

(14) Rangwala, H. A.; Morrell, B. R.; Mather, A. E.; Otto, F. D. Absorption of CO_2 into aqueous tertiary amine/mea solutions. *Can. J. Chem. Eng.* **1992**, *70*, 482−490.

(15) Inoue, S.; Itakura, T.; Nakagaki, T.; Furukawa, Y.; Sato, H.; Yamanaka, Y. Experimental study on CO_2 solubility in aqueous piperazine/alkanolamines solutions at stripper conditions. *Energy Procedia* **2013**, *37*, 1751−1759.

(16) Aghel, B.; Janati, S.; Wongwises, S.; Shadloo, M. S. Review on CO_2 capture by blended amine solutions. *Int. J. Greenhouse Gas Control* **2022**, *119*, 103715.

(17) Sema, T.; Naami, A.; Fu, K.; Edali, M.; Liu, H.; Shi, H.; Liang, Z.; Idem, R.; Tontiwachwuthikul, P. Comprehensive mass transfer and reaction kinetics studies of CO_2 absorption into aqueous solutions of blended MDEA-MEA. *Chem. Eng. J.* **2012**, *209*, 501−512.

(18) Zhang, R.; Zhang, X.; Yang, Q.; Yu, H.; Liang, Z.; Luo, X. Analysis of the reduction of energy cost by using MEA-MDEA-PZ solvent for post-combustion carbon dioxide capture (PCC). *Appl. Energy* **2017**, *205*, 1002−1011.

(19) Zhang, J.; Qiao, Y.; Agar, D. W. Improvement of lipophilic-amine-based thermomorphic biphasic solvent for energy-efficient carbon capture. *Energy Procedia* **2012**, *23*, 92−101.

(20) Liu, F.; Fang, M.; Yi, N.; Wang, T. Research on alkanolamine-based physical-chemical solutions as biphasic solvents for CO_2 capture. *Energy Fuels* **2019**, *33*, 11389−11398.

(21) Xu, G.-W.; Zhang, C.-F.; Qin, S.-J.; Gao, W.-H.; Liu, H.-B. Gas-liquid equilibrium in a CO_2-MDEA-H_2O system and the effect of piperazine on it. *Ind. Eng. Chem. Res.* **1998**, *37*, 1473−1477.

(22) Svensson, H.; Hulteberg, C.; Karlsson, H. T. Heat of absorption of CO_2 in aqueous solutions of N-methyldiethanolamine and piperazine. *Int. J. Greenhouse Gas Control* **2013**, *17*, 89−98.

(23) Mudhasakul, S.; Ku, H.-m.; Douglas, P. L. A simulation model of a CO_2 absorption process with methyldiethanolamine solvent and piperazine as an activator. *Int. J. Greenhouse Gas Control* **2013**, *15*, 134−141.

(24) Zhao, B.; Liu, F.; Cui, Z.; Liu, C.; Yue, H.; Tang, S.; Liu, Y.; Lu, H.; Liang, B. Enhancing the energetic efficiency of MDEA/PZ-based CO_2 capture technology for a 650 MW power plant: process improvement. *Appl. Energy* **2017**, *185*, 362−375.

(25) Khan, B. A.; Ullah, A.; Saleem, M. W.; Khan, A. N.; Faiq, M.; Haris, M. Energy minimization in piperazine promoted MDEA-based CO_2 capture process. *Sustainability* **2020**, *12*, 8524.

(26) Le Moullec, Y.; Neveux, T.; Al Azki, A.; Chikukwa, A.; Hoff, K. A. Process modifications for solvent-based post-combustion CO_2 capture. *Int. J. Greenhouse Gas Control* **2014**, *31*, 96−112.

(27) Sharma, M.; Qadir, A.; Khalilpour, R.; Abbas, A. Modeling and analysis of process configurations for solvent-based post-combustion carbon capture. *Asia-Pac. J. Chem. Eng.* **2015**, *10*, 764−780.

(28) Li, K.; Cousins, A.; Yu, H.; Feron, P.; Tade, M.; Luo, W.; Chen, J. Systematic study of aqueous monoethanolamine-based CO_2 capture process: model development and process improvement. *Energy Sci. Eng.* **2016**, *4*, 23−39.

(29) Mostafavi, E.; Ashrafi, O.; Navarri, P. Assessment of process modifications for amine-based post-combustion carbon capture processes. *Clean. Eng. Technol.* **2021**, *4*, 100249.

(30) Cousins, A.; Wardhaugh, L. T.; Feron, P. H. M. A survey of process flow sheet modifications for energy efficient CO_2 capture from flue gases using chemical absorption. *Int. J. Greenhouse Gas Control* **2011**, *5*, 605−619.

(31) Li, T.; Yang, C.; Tantikhajorngosol, P.; Sema, T.; Liang, Z.; Tontiwachwuthikul, P.; Liu, H. Comparative desorption energy consumption of post-combustion CO_2 capture integrated with mechanical vapor recompression technology. *Sep. Purif. Technol.* **2022**, *294*, 121202.

(32) Liu, L.; Wang, S.; Niu, H.; Gao, S. Process and integration optimization of post-combustion CO_2 capture system in a coal power plant. *Energy Procedia* **2018**, *154*, 86−93.

(33) Li, X.; Wang, S.; Chen, C. Experimental study of energy requirement of CO_2 desorption from rich solvent. *Energy Procedia* **2013**, *37*, 1836−1843.

(34) Aronu, U. E.; Gondal, S.; Hessen, E. T.; Haug-Warberg, T.; Hartono, A.; Hoff, K. A.; Svendsen, H. F. Solubility of CO_2 in 15, 30, 45 and 60 mass% MEA from 40 to 120 °C and model representation using the extended UNIQUAC framework. *Chem. Eng. Sci.* **2011**, *66*, 6393−6406.

https://doi.org/10.1021/acs.energyfuels.3c04115
Energy Fuels 2024, 38, 2129−2140

(35) Zhao, R.; Zhang, Y.; Zhang, S.; Li, Y.; Han, T.; Gao, L. The full chain demonstration project in China—status of the CCS development in coal-fired power generation in GuoNeng Jinjie. *Int. J. Greenhouse Gas Control* **2021**, *110*, 103432.
(36) Liu, Y.; Li, H.; Wei, G.; Zhang, H.; Li, X.; Jia, Y. Mass transfer performance of CO_2 absorption by alkanolamine aqueous solution for biogas purification. *Sep. Purif. Technol.* **2014**, *133*, 476−483.
(37) Lin, S. H.; Shyu, C. T. Performance characteristics and modeling of carbon dioxide absorption by amines in a packed column. *Waste Manage.* **1999**, *19*, 255−262.
(38) Oexmann, J.; Kather, A. Minimising the regeneration heat duty of post-combustion CO_2 capture by wet chemical absorption: the misguided focus on low heat of absorption solvents. *Int. J. Greenhouse Gas Control* **2010**, *4*, 36−43.
(39) Kim, I.; Hoff, K. A.; Hessen, E. T.; Haug-Warberg, T.; Svendsen, H. F. Enthalpy of absorption of CO_2 with alkanolamine solutions predicted from reaction equilibrium constants. *Chem. Eng. Sci.* **2009**, *64*, 2027−2038.
(40) Jiang, K.; Li, K.; Yu, H.; Chen, Z.; Wardhaugh, L.; Feron, P. Advancement of ammonia based post-combustion CO_2 capture using the advanced flash stripper process. *Appl. Energy* **2017**, *202*, 496−506.
(41) Jiang, K.; Li, K.; Yu, H.; Feron, P. H. M. Piperazine-promoted aqueous-ammonia-based CO_2 capture: process optimization and modification. *Chem. Eng. J.* **2018**, *347*, 334−342.
(42) Lin, Y.-J.; Madan, T.; Rochelle, G. T. Regeneration with rich bypass of aqueous piperazine and monoethanolamine for CO_2 capture. *Ind. Eng. Chem. Res.* **2014**, *53*, 4067−4074.
(43) Liu, C.; Shao, L.; Pan, C.; Xu, F.; Wu, Z.; Zhao, Z.; Chen, Y.; Fan, H.; Zheng, C.; Gao, X. Multi-stage solvent circulation absorption enhancement: system optimization for energy-saving CO_2 capture. *Sep. Purif. Technol.* **2024**, *332*, 125644.
(44) Shao, L.; Liu, C.; Wang, Y.; Yang, Z.; Wu, Z.; Zhao, Z.; Teng, W.; Hu, D.; Zheng, C.; Gao, X. Reducing aerosol emissions by decoupled parameter management during the CO_2 capture process in a multi-stage circulation absorber. *Environ. Sci. Technol.* **2023**, *57*, 10467−10477.
(45) Ayittey, F. K.; Saptoro, A.; Kumar, P.; Wong, M. K. Energy-saving process configurations for monoethanolamine-based CO_2 capture system. *Asia-Pac. J. Chem. Eng.* **2020**, *16*, No. e2576.
(46) Ali, B. S.; Aroua, M. K. Effect of piperazine on CO_2 loading in aqueous solutions of MDEA at low pressure. *Int. J. Thermophys.* **2004**, *25*, 1863−1870.
(47) Kierzkowska-Pawlak, H. Enthalpies of absorption and solubility of CO_2 in aqueous solutions of methyldiethanolamine. *Sep. Sci. Technol.* **2007**, *42*, 2723−2737.
(48) Abu-Zahra, M. R. M.; Schneiders, L. H. J.; Niederer, J. P. M.; Feron, P. H. M.; Versteeg, G. F. CO_2 capture from power plants: Part I. A parametric study of the technical performance based on monoethanolamine. *Int. J. Greenhouse Gas Control* **2007**, *1*, 37−46.
(49) Notz, R.; Mangalapally, H. P.; Hasse, H. Post combustion CO_2 capture by reactive absorption: pilot plant description and results of systematic studies with MEA. *Int. J. Greenhouse Gas Control* **2012**, *6*, 84−112.
(50) Warudkar, S. S.; Cox, K. R.; Wong, M. S.; Hirasaki, G. J. Influence of stripper operating parameters on the performance of amine absorption systems for post-combustion carbon capture: Part I. High pressure strippers. *Int. J. Greenhouse Gas Control* **2013**, *16*, 342−350.
(51) Adeosun, A.; Abu-Zahra, M. R. M. Evaluation of amine-blend solvent systems for CO_2 post-combustion capture applications. *Energy Procedia* **2013**, *37*, 211−218.
(52) Li, K.; Leigh, W.; Feron, P.; Yu, H.; Tade, M. Systematic study of aqueous monoethanolamine (MEA)-based CO_2 capture process: techno-economic assessment of the MEA process and its improvements. *Appl. Energy* **2016**, *165*, 648−659.

https://doi.org/10.1021/acs.energyfuels.3c04115
Energy Fuels 2024, 38, 2129−2140